



UNIVERSITY OF LEEDS

This is a repository copy of *Progressive Development of Aberrant Smooth Muscle Cell Phenotype in Abdominal Aortic Aneurysm Disease*.

White Rose Research Online URL for this paper:
<http://eprints.whiterose.ac.uk/125628/>

Version: Accepted Version

Article:

Riches, K, Clark, E, Helliwell, RJ et al. (6 more authors) (2018) Progressive Development of Aberrant Smooth Muscle Cell Phenotype in Abdominal Aortic Aneurysm Disease. *Journal of Vascular Research*, 55 (1). pp. 35-46. ISSN 1018-1172

<https://doi.org/10.1159/000484088>

(c) 2018, S. Karger AG, Basel. This is the peer-reviewed but unedited manuscript version of the following article: 'Riches, K, Clark, E, Helliwell, RJ et al. (2018) Progressive Development of Aberrant Smooth Muscle Cell Phenotype in Abdominal Aortic Aneurysm Disease. *Journal of Vascular Research*, 55 (1). pp. 35-46.' The final, published version is available at <https://doi.org/10.1159/000484088>.

Reuse

Items deposited in White Rose Research Online are protected by copyright, with all rights reserved unless indicated otherwise. They may be downloaded and/or printed for private study, or other acts as permitted by national copyright laws. The publisher or other rights holders may allow further reproduction and re-use of the full text version. This is indicated by the licence information on the White Rose Research Online record for the item.

Takedown

If you consider content in White Rose Research Online to be in breach of UK law, please notify us by emailing eprints@whiterose.ac.uk including the URL of the record and the reason for the withdrawal request.



eprints@whiterose.ac.uk
<https://eprints.whiterose.ac.uk/>

Progressive development of aberrant smooth muscle cell phenotype in abdominal aortic aneurysm disease

Kirsten Riches PhD^{1,2}, Emily Clark PhD^{3,4}, Rebecca J Helliwell BSc¹, Timothy G Angelini MBChB⁵, Karen E Hemmings PhD^{1,4}, Marc A Bailey PhD^{1,4,6}, Katherine I Bridge PhD^{1,4,6}, D Julian A Scott FRCS Ed^{1,4,6}, Karen E Porter PhD^{1,4*}

¹Leeds Institute of Cardiovascular and Metabolic Medicine (LICAMM), University of Leeds, Leeds, UK

²Faculty of Life Sciences, University of Bradford, Bradford, UK

³Institute of Medical and Biological Engineering, School of Mechanical Engineering, University of Leeds, Leeds, UK

⁴Multidisciplinary Cardiovascular Research Centre (MCRC), University of Leeds, Leeds, UK

⁵Royal London Hospital, Whitechapel, London, UK

⁶Leeds Vascular Institute, Leeds General Infirmary, Leeds, UK

Running title: Aberrant SMC in aneurysmal disease

* To whom correspondence should be addressed: Dr Karen E. Porter, Institute of Cardiovascular and Metabolic Medicine, LIGHT Laboratories, Clarendon Way, University of Leeds, Leeds LS2 9JT, UK. Tel: +44(0)113-3434806. Fax: +44(0)113-3434803. E-mail: k.e.porter@leeds.ac.uk

Abstract

Abdominal aortic aneurysm (AAA) is a silent, progressive disease with high mortality and increasing prevalence with aging. Smooth muscle cell (SMC) dysfunction contributes to gradual dilatation and eventual rupture of the aorta. Here we studied phenotypic characteristics in SMC cultured from end-stage human AAA ($\geq 5\text{cm}$) and cells cultured from a porcine carotid artery (PCA) model of early and end-stage aneurysm.

Human AAA-SMC presented a secretory phenotype and expressed elevated levels of differentiation marker miR-145 (2.2-fold, $P < .001$) and senescence marker SIRT-1 (1.3-fold, $P < .05$), features not recapitulated in aneurysmal PCA-SMC. Human and end-stage porcine aneurysmal cells were frequently multi-nucleated (3.9-fold, $P < .001$ and 1.8-fold, $P < .01$ respectively, versus control cells) and displayed aberrant nuclear morphology. Human AAA-SMC exhibited higher levels of the DNA damage marker γH2AX (3.9-fold, $P < .01$ vs. control SMC). These features did not correlate with patients' chronological age; and are therefore potential markers for pathological premature vascular aging. Early-stage PCA-SMC (control and aneurysmal) were indistinguishable from one another across all parameters.

The principal limitation of human studies is tissue availability only at end-stage disease.

Refinement of a porcine bioreactor model would facilitate study of temporal modulation of SMC behaviour during aneurysm development and potentially identify therapeutic targets to limit AAA progression.

Key words: Abdominal aortic aneurysm; human; porcine; smooth muscle cells; aging; DNA damage; senescence; in vitro.

Introduction

Abdominal aortic aneurysm (AAA) is a progressive, generally asymptomatic dilatation of the aorta affecting ~5.5% of the population. Risk factors for AAA include male gender, increasing age and smoking [1]. Rupture is associated with a high mortality risk of 60-70%; consequently, national screening programmes have been established to detect AAA in men over the age of 65 [1]. Elective open or endovascular repair is then offered when the risks of intervention are outweighed by the annual risk of rupture, which is correlated with AAA size.

AAA is a multi-factorial disease. The pro-inflammatory infiltration of the aorta by immune cells such as macrophages and lymphocytes has been recognised for many years and has consequently been the focus of intensive research [2]. In addition to the inflammatory component, AAA is characterised by progressive decline in the number of smooth muscle cells (SMC) within the aortic wall [3], and degradation of extracellular matrix (ECM) through the production of matrix metalloproteinases (MMPs) [4]. In combination, this weakens the structural integrity of the aorta, rendering it more susceptible to rupture.

SMC are the principal cellular component of the vascular wall and they play essential roles in maintaining vessel architecture and remodelling in response to environmental stimuli. They do this through switching between contractile (differentiated) and synthetic (dedifferentiated) phenotypes [5]. Whilst this plasticity is essential to adaptive remodelling, it is also implicated in the development of human AAA [6-9] and animal models of abdominal and thoracic aneurysm [6, 10]. Undeniably the involvement of SMC in AAA progression is an area worthy of research, however the key challenge facing investigators is that human tissue is accessible only at end-stage disease. Whilst animal models are undoubtedly of great value in AAA research, they do not fully recapitulate the clinical scenario in man as they are most commonly artificially induced via treatment with angiotensin II, calcium chloride or elastase, or mechanically induced using balloon angioplasty [11]. As such, they benefit from being complemented with alternative models.

SMC isolated from end-stage human tissue exhibit diverse features in culture [7-9]. Recently, we described a distinct SMC phenotype isolated from end-stage human AAA tissue (aortic diameter ≥ 5 cm) characterised by a large rhomboid morphology, slow proliferative rate, increased senescence and reduced levels of secreted MMP-2 compared to SMC cultured from non-aneurysmal human saphenous vein (SV) [9]. Furthermore, we established a novel ex vivo bioreactor model whereby porcine carotid arteries (PCA) were briefly treated with a combination of collagenase and elastase (CCE) or control vehicle gel (VEH), then maintained under flow for 12 days in a bioreactor. During this time, dilatation of the vessel was apparent and importantly, CCE-SMC derived from the vessels retrieved at the end of the culture period were compatible with those of end-stage human AAA-SMC with respect to morphology and behaviour in culture [9]. There is clearly a demand for models that may help identify factors that precede aneurysm development in order to find targets for new therapeutics.

The risk of AAA increases with age [1], however the effects of aging on SMC are controversial with multiple conflicting reports regarding its influence on SMC proliferation, migration and inflammation (recently reviewed in [12]). Some of the phenotypic features of AAA-SMC that we have described, namely aberrant morphology, increased senescence and poor proliferative capacity [9] correspond to features apparent in aged SMC [13], however our observation of reduced MMP-2 secretion is at variance with animal models of aging [14]. Aging is associated with increased production of proinflammatory cytokines [15] and the development of cellular senescence, which has a multitude of effects on cell phenotype and behaviour [16]. We hypothesised that human AAA-SMC and porcine CCE-SMC would display features consistent with a premature aging phenotype. Consequently, the purpose of this study was to perform a detailed side-by-side comparison of human AAA-SMC and porcine CCE-SMC. Cells were explored in terms of morphology, expression of markers associated with aging and senescence (sirtuin-1, -3 and -6, miR-145), and evaluation of DNA

damage (γ H2AX). In a further series of experiments, we also examined these features in porcine cells cultured from vessels maintained in the bioreactor for a shorter interval (3 days) to explore the temporal nature of aneurysm pathology.

Methods

Human cell isolation

Human SMC were isolated using an explant technique as previously described [17].

Aneurysmal (AAA) SMC were isolated from tissue fragments from patients undergoing open surgical repair, and non-aneurysmal SMC were isolated from SV or internal mammary artery (IMA) of patients undergoing coronary artery bypass grafting. Mean aneurysm diameter was 6.48 ± 0.22 (range 4.9 - 9.5) cm. All procedures were performed at the Leeds General Infirmary. Approval of the experimental protocol was given by Leeds West Research Ethics Committee (ref CA/01/040) and all patients gave informed, written consent. The study conformed to the Declaration of Helsinki. Following explant, established SMC were maintained in Dulbeccos's Modified Eagle Medium (DMEM) supplemented with 10% foetal calf serum (FCS), 1% L-Glutamine and 1% penicillin/streptomycin fungizone (full growth medium, FGM) at 37°C in 5% CO₂ in air and serially passaged using trypsin/EDTA as necessary. All experiments were performed on cells between passages 3-6.

Bioreactor and porcine cell isolation

Porcine carotid arteries (PCA) were harvested from four month old, 65kg animals as previously described [9]. All procedures were performed according to UK Home Office regulations. Isolated vessels were treated with control gel (VEH) or gel containing collagenase and elastase (CCE), to induce an aneurysm-like dilatation of the vessel and maintained in a bioreactor under flow for 12 days (classified as 'end stage'), as previously

described [9] or 3 days (classified as 'early stage'). SMC were subsequently explanted from the retrieved vessels and maintained in FGM. As for human SMC, experiments were performed on early passage cells (3-6).

Light microscopy

Sub-confluent cells in FGM were imaged under phase at x100 magnification to examine any visible cytoskeletal and ultra-structural features. For quantification of multi-nucleation, multiple fields of view were acquired and the number of nuclei in ~150 individual cells were enumerated. Multi-nucleated cells were represented as a proportion of the total number of cells examined.

Immunocytochemistry

Cells were cultured on glass coverslips in FGM for 96h prior to fixation in 4% paraformaldehyde. The F-actin cytoskeleton was visualised using rhodamine phalloidin as previously described [18]. Both low (x200) and high magnification (x630) images were taken in multiple fields using a LSM510 Upright confocal microscope.

To examine nuclear morphology, five random fields of view were imaged for each DAPI-stained cell population at x400 magnification. Nuclei were classified as 'normal' (ovoid) or 'aberrant' (irregular with blebbing, or apoptotic), and the proportion of aberrant nuclei calculated. To aid the distinction between the two classifications, DAPI was visualised in yellow to give a clear contrast.

For quantification of γ H2AX-positive nuclei, cells were stained with primary γ H2AX antibody (1:100) overnight followed by Cy3-conjugated donkey anti-rabbit secondary antibody (1:400) for 3 h at room temperature before mounting using ProLong Gold containing DAPI nuclear stain. Five random fields of view were captured from each cell

population at x200 magnification. Data were expressed as the proportion of γ H2AX-positive nuclei (pink) relative to the total number of nuclei (blue and pink).

RNA isolation and RT-PCR

RNA was isolated from cells cultured in FGM and reverse transcribed as previously described [19]. Expression of SIRT-1, SIRT-3 and SIRT-6 in human and porcine cells was determined using specific TaqMan assays and expressed as a percentage of GAPDH.

For miR-145, RNA was reverse transcribed as previously described [20] and expression of human and porcine miR-145 determined using specific TaqMan assays and expressed as a percentage of short ribonuclear RNA, U6.

Statistical analyses

Data are expressed as mean \pm SEM with n representing the number of experiments on cells from different patients or animals. Statistical analysis was performed using GraphPad Prism and ratio t-tests, one-way ANOVA with Newman-Keuls post-hoc test as appropriate.

Correlative data was tested for normality using D'Agostino and Pearson omnibus test and any associations identified using Spearman or Pearson correlation as appropriate. Correlation between different factors is indicated by r. P<.05 was considered statistically significant.

Results

SMC morphology

AAA-SMC frequently presented perinuclear granulation; a feature seldom observed in non-aneurysmal SV or IMA-SMC (Fig. 1A). Most strikingly, AAA-SMC often exhibited a defined, fragmented cytoskeleton that was clearly visible under light microscopy (Fig. 1A).

We examined the cytoskeleton in more detail using rhodamine phalloidin to stain F-actin fibres. Low magnification images (x200) were used to illustrate that staining was apparent in

all cells within the population, and high magnification images (x630) were obtained to visualise the organisation of F-actin fibres in greater detail. Substantial fragmentation was evident under both low and high power magnification in AAA-SMC, in contrast to long, parallel F-actin fibres that were visible in SV-SMC (Fig. 1B) and in IMA-SMC [21].

As previously noted, porcine SMC were smaller than human SMC [9] making perinuclear granulation and the cytoskeleton more difficult to decipher using light microscopy, although they were visible to a degree. There was no apparent difference in granulation or cytoskeletal prominence in any early stage CCE-SMC (Fig. 1C), and F-actin fibres were maintained in an ordered configuration resembling those of VEH-SMC (Fig. 1D). In contrast, there was clear evidence of perinuclear granulation in end stage CCE-SMC and disruption to the cytoskeleton which was not evident in VEH-SMC (Fig. 1E); an observation that was exemplified using immunofluorescence (Fig. 1F).

Senescence markers

AAA-SMC expressed SIRT-1, -3 and -6, and had significantly lower expression of SIRT-1 compared to SV-SMC but not IMA-SMC (Fig. 2A). SIRT-3 and SIRT-6 were not different between the groups. SIRT-6 expression levels were consistently lower than SIRT-1 and SIRT-3 regardless of SMC source (Fig. 2A).

The reduced expression of SIRT-1 in AAA-SMC was not replicated in porcine SMC. In early stage CCE-SMC, SIRT-1 expression was comparable to VEH-SMC in two out of the three vessels studied, however the third vessel had a higher expression of SIRT-1 in the VEH-SMC. This skewed the data yet, it still remains non-significant ($P=0.494$, Fig. 2C). SIRT-3 was also unaffected by CCE treatment (Fig. 2C). In end stage experiments, there were no significant differences between CCE-SMC and VEH-SMC (Fig. 2D). Expression of SIRT-1 and SIRT-3 was routinely higher in porcine SMC (by 2.6- and 2.1-fold respectively) than in

human cells; although expression of SIRT-6 was undetectable in all porcine RNA samples (data not shown).

Expression levels of miR-145 in AAA-SMC were >2-fold higher than in non-aneurysmal cells (57.4% vs. 26.0% in SV-SMC and 20.5% in IMA-SMC; Fig. 2B). However, we did not see this variance in porcine cells (neither early nor end stage) where overall expression levels were similar between all CCE- and VEH-SMC (Fig. 2E-F).

Given that SV- and IMA-SMC were phenotypically comparable (Fig. 1, 2) we subsequently used SV-SMC as a non-aneurysmal comparator for the remainder of the study due to ready availability of primary tissue and consistency with our published report [9].

Markers of DNA damage

AAA-SMC exhibited a higher frequency of multi-nucleation than SV-SMC, with 7.4% of cells containing two or more nuclei (Fig. 3A). In contrast, only 1.8% of SV-SMC were multi-nucleated (Fig. 3A). AAA-SMC also had a greater proportion of aberrant nuclei (18.5%) compared to 7.6% in SV-SMC (Fig. 3B). Furthermore, 32.4% of AAA-SMC stained positively for γ H2AX compared with only 8.3% in SV-SMC (Fig. 3C).

Early stage SMC demonstrated a modest elevation in the proportion of multi-nucleated cells compared with end stage cells, either human or porcine. However, there was no difference between VEH- versus CCE-SMC at this time point (Fig. 3D). Consistent with this, there were few aberrant nuclei in either group (Fig. 3E). In early stage experiments, γ H2AX positive nuclei were frequent although the degree of DNA damage was minor, as evidenced by few positive foci per nucleus (Fig. 3F).

In contrast, there was divergent multi-nucleation and aberrant nuclei in end-stage porcine SMC which was significantly elevated in CCE-SMC (Fig.3G, H). There was a trend towards

a greater number of H2AX-positive nuclei in CCE-SMC, and these exhibited a higher degree of DNA damage with multiple foci (Fig. 3I).

Association of experiments with age

SMC were isolated from surgical samples acquired from a total of 31 patients undergoing AAA open repair (mean age 72.6 ± 1.1 years, range 67-87 years, 93% male) and from the SV from a total of 57 patients harvested sequentially during coronary artery bypass grafting (mean age 62.6 ± 1.5 years, range 40-83 years, 89% male; $P < .001$, Fig. 5A).

In order to determine whether chronological patient age accounted for the differences we observed, we performed correlative analysis for chronological age in both the AAA and SV groups. Here, analysis was performed specifically on the subset of patient cells that were used for each particular experiment. Cells were selected for experimental use chronologically and not preselected according to clinical or cell behavioural data. This investigation revealed that patient donor age was not significantly correlated to SIRT-1 or miR-145 expression (Fig. 5B-C), the number or morphology of nuclei (Fig. 5D-E) or the degree of γ H2AX positivity (Fig. 5F). We propose that these features are therefore markers of pathological, vascular aging rather than attributable to the age of the patient donor.

Discussion

AAA disease is a significant healthcare problem with high mortality from rupture. The present study builds on our previous work demonstrating that end-stage AAA-SMC and porcine CCE-SMC are significantly larger than non-aneurysmal controls [9] and has revealed for the first time that SMC derived from both human end-stage AAA tissue and ex vivo protease-treated porcine arteries maintained under flow, exhibit features consistent with

premature aging and increased DNA damage. This could conceivably underlie, at least in part, their impaired functionality.

The morphological characteristics of aneurysmal SMC (both human and end-stage CCE) were distinct, comprising a large spread cell area and rhomboid morphology [9]. Importantly, aberrant morphology was apparent in cells emerging early from primary explants (data not shown). All experiments in this study and in our previous report [9] were performed on early passage cells (p3-p6), an interval over which we have confirmed that morphological characteristics are retained [21]. In the current study, we have extended our morphological characterisation by noting marked aberrations in the F-actin cytoskeleton. Similar F-actin features – namely, truncated and disorganised fibres – have also been described in SV-SMC from patients with Type 2 diabetes (T2DM) [22, 20, 21]. As both aneurysm disease and T2DM are considered to be conditions characterised by premature aging [23, 24] it is feasible that disorganisation of F-actin in SMC is a feature of aged cells, rather than representative of a particular disease pathology per se.

SMC are highly plastic and can switch between differentiated, contractile and dedifferentiated, synthetic phenotypes which is essential to their function [5]. The synthetic phenotype is characterised by morphological changes including adoption of a rhomboid appearance, myofilament loss and an increase in synthetic organelles including Golgi apparatus and rough endoplasmic reticulum [5]. Whilst we did not investigate markers of secretory organelles it is likely that the perinuclear granulation we observed in the human and end-stage porcine aneurysmal cells, in combination with aberrant cell morphology and disorganisation of the cytoskeleton, are indicative of a switch towards a secretory phenotype. It has been suggested that this could be an artefact caused by the *in vitro* nature of this study, and could have been induced due to differences in cell size or proliferative capacity that we have previously described [9]. AAA-SMC are undeniably larger than SV-SMC in culture and

have a slower proliferative rate [9], however their size and impaired proliferative capacity are comparable with our documented phenotypic characterisation of IMA-SMC [21]. In the present study, a substantially higher proportion of AAA-SMC exhibited ‘secretory’ features compared to IMA-SMC (Fig. 1A/B), asserting that our observations are not due to in vitro conditions but instead are related to their previous in vivo environment.

Cells that permanently withdraw from the cell cycle adopt a senescence-associated secretory phenotype (SASP) characterised by secretion of various mediators, typically IL-1, IL-6, IL-8 and monocyte chemoattractant protein (MCP)-1 [16]. These secreted factors can induce senescence in neighbouring cells via paracrine/autocrine mechanisms, a phenomenon known as a ‘bystander effect’ [25]. AAA-SMC exhibit telomere attrition [26] and we previously demonstrated that aneurysmal SMC exhibit a greater degree of senescence, indicated by β -galactosidase staining [9]. We therefore examined the expression of sirtuins; longevity proteins whose expression is inversely correlated with cell age [27]. Indeed SIRT-1, via a p53-dependent mechanism, can promote DNA repair and regulate the cell cycle, thereby promoting viability and longevity [28]. Whilst lower expression levels of SIRT-1 in AAA-SMC compared to non-aneurysmal SV-SMC supports our hypothesis of premature aging, this was not a feature replicated in the porcine model (either early or end-stage) nor in IMA-SMC, suggesting that SIRT-1 expression may be inherently variable between vascular beds.

However, basal expression levels of SIRT-1 in porcine SMC were 2.6-4.9-fold higher than corresponding expression levels in human SMC, supporting the concept that the porcine cells were physiologically ‘younger’ than the end-stage human cells. In patients with AAA, dilation progresses over many years [29]. In order to induce a temporally aged porcine model that more accurately mirrors the human condition, it seems likely that culture in the bioreactor over an extended period is necessary, whilst providing conditions that are able to maintain vessel viability throughout.

MiR-145 is highly expressed in SMC and is involved in differentiation [24] and is reportedly dysregulated in a number of cardiovascular pathologies [21, 25]. miR-145 is an important regulator of vascular SMC phenotype, and we demonstrated its role in driving phenotypic change in human SV-SMC. Specifically, over-expression of miR-145 caused cells to become large and spread, disrupted the F-actin cytoskeleton, and reduced proliferation. This previous report also discovered elevated levels of miR-145 in native T2DM-SMC compared to non-diabetic SV, which was maintained throughout serial passaging [20]. Importantly, this elevation was observed in age-matched patients which strengthens the notion that miR-145 is unlikely to be related to donor age. Our data presented here and previously [9] indicate that an enlarged, slowly proliferating cell phenotype is common to both AAA-SMC and T2DM-SMC. Here we observed elevated levels (2.2-fold) of miR-145 relative to venous and arterial non-aneurysmal SMC. Interestingly, expression of miR-145 is reportedly elevated in ascending aortic aneurysm tissue [30]. Increasing age is a key risk factor for the development of AAA, which is most prevalent in males over the age of 65 years [1], and premature vascular aging is also considered to underlie the development of cardiovascular complications in T2DM [31]. SV-SMC from T2DM patients express miR-145 at levels comparable to those described here in AAA-SMC [20]; it is therefore conceivable that miR-145 serves as a marker of prematurely aged vascular SMC in general, and is not necessarily specific to a particular pathology. In the bioreactor, where the time course of vessel dilatation is accelerated, it is unlikely that porcine cells undergo a comparable sequential disease process following the application of CCE.

A key driver of cellular aging is DNA damage, whereby cells temporarily withdraw from the cell cycle and undergo DNA repair to prevent mutations in future generations. When DNA damage is overwhelming to a degree that exceeds the capacity of the cell to undergo DNA repair, permanent withdrawal from the cell cycle and senescence or apoptosis ensues [32].

Multi-nucleation and nuclear deformation are features of sustained DNA damage and aging [13, 27] and further, phosphorylation of histone H2AX (γ H2AX) is an early event in double-stranded DNA damage signalling [28]. Our current and previous data demonstrate conclusively that aneurysmal SMC are senescent [9], therefore it was logical to explore any evidence of persistent DNA damage. We examined multi-nucleation (a feature of senescent and damaged cells [33, 34]), deformation of normal ovoid nuclear morphology (more common in aged and DNA damaged cells [35, 13]) and the presence of γ H2AX (an early event in double-stranded DNA damage [36]). Our results show unequivocally that human AAA-SMC exhibit a greater extent of DNA damage than non-aneurysmal SMC, in agreement with a previous study that also examined γ H2AX and 8-dihydro-8-oxo-2'-deoxyguanosine as a marker of oxidative DNA damage [26]. However, in that study AAA-SMC were explored in situ in tissue sections, or isolated as primary cells by a cytopsin method without culturing [26]. It is notable that in early-stage PCA-SMC, the presence of multi-nucleation was high in both VEH- and CCE-SMC alike. This was paralleled by a higher proportion of γ H2AX-positive cells in both groups, however these cells exhibited few foci in each nucleus compared with either human or porcine end stage aneurysmal cells (Fig. 3C, F, I). It could be argued that the procedure of preparing and placing vessels in the bioreactor induces transient and reversible DNA damage although this would require additional corroboration.

Persistence of DNA damage throughout culture and passaging is likely explained by the existence of epigenetic mechanisms. A number of microRNAs are known to regulate proteins involved in the DNA damage response pathway, for example miR-421 (targets ATM), miR-24 (targets H2AX) and miR-125b (targets p53). Furthermore, activation of the DNA damage response up-regulates transcription and processing of a further subset of miRNAs including miR-34, miR-145 and miR-215 (reviewed in [37]). In the present study we observed persistent

DNA damage in porcine cells without elevated levels of miR-145, therefore it is unlikely that miR-145 is a causative factor of the DNA damage we observe in both human and porcine aneurysmal SMC. miR-24 reportedly inhibits SMC proliferation [38] and miR-34 is up-regulated in senescent SMC [39]; these are worthy of investigation and may represent promising candidates for future research.

In summary, our data support the notion that end-stage aneurysmal SMC (both human and porcine) exhibit characteristics consistent with DNA damage and a senescence associated secretory phenotype. These features are not present in early-stage porcine SMC, suggesting that they are imparted later in the temporal progression of aneurysm development. Identifying the critical time point where DNA damage can first be detected may provide opportunities to develop interventions which could prevent or even reverse this damage. In this respect, application of a further interim time point in the bioreactor could provide an opportunity for evaluating potential therapeutic agents, introduced early and evaluated for efficacy at the later times. In the longer term, these data may lead to development of new pharmacological interventions for AAA in man.

Acknowledgements

This study was supported in part by a grant from the Leeds Teaching Hospitals Charitable Foundation (9R11/8002) to DJA Scott. Timothy Angelini received an Intercalated Bachelor of Science Degree in Surgery Award from the Royal College of Surgeons of England (2010-11). Rebecca Helliwell was a recipient of a Wolfson Scholarship and an Intercalated Bachelor of Science Degree in Surgery Award from the Royal College of Surgeons of England (2016-17).

References

1. Erbel R, Aboyans V, Boileau C, Bossone E, Bartolomeo RD, Eggebrecht H, Evangelista A, Falk V, Frank H, Gaemperli O, Grabenwoger M, Haverich A, Jung B, Manolis AJ, Meijboom F, Nienaber CA, Roffi M, Rousseau H, Sechtem U, Sirnes PA, Allmen RS, Vrints CJ: 2014 ESC Guidelines on the diagnosis and treatment of aortic diseases: Document covering acute and chronic aortic diseases of the thoracic and abdominal aorta of the adult. The Task Force for the Diagnosis and Treatment of Aortic Diseases of the European Society of Cardiology (ESC). *Eur. Heart J* 2014;35(41):2873-2926
2. McCormick ML, Gavrilu D, Weintraub NL: Role of oxidative stress in the pathogenesis of abdominal aortic aneurysms. *Arterioscler. Thromb. Vasc. Biol.* 2007;27(3):461-469
3. Lopez-Candales A, Holmes DR, Liao S, Scott MJ, Wickline SA, Thompson RW: Decreased vascular smooth muscle cell density in medial degeneration of human abdominal aortic aneurysms. *Am. J. Pathol.* 1997;150(3):993-1007
4. Theruvath TP, Jones JA, Ikonomidis JS: Matrix metalloproteinases and descending aortic aneurysms: parity, disparity, and switch. *J. Card. Surg.* 2012;27(1):81-90
5. Owens GK, Kumar MS, Wamhoff BR: Molecular regulation of vascular smooth muscle cell differentiation in development and disease. *Physiol. Rev.* 2004;84(3):767-801
6. Ailawadi G, Moehle CW, Pei H, Walton SP, Yang Z, Kron I, Lau CL, Owens GK: Smooth muscle phenotypic modulation is an early event in aortic aneurysms. *The J. Thorac. Cardiovasc. Surg.* 2009;138(6):1392-1399
7. Airhart N, Brownstein BH, Cobb JP, Schierding W, Arif B, Ennis TL, Thompson RW, Curci JA: Smooth muscle cells from abdominal aortic aneurysms are unique and can independently and synergistically degrade insoluble elastin. *J. Vasc. Surg.* 2014;60(4):1033-1041
8. Liao S, Curci JA, Kelley BJ, Sicard GA, Thompson RW: Accelerated replicative senescence of medial smooth muscle cells derived from abdominal aortic aneurysms compared to the adjacent inferior mesenteric artery. *J. Surg. Res.* 2000;92(1):85-95
9. Riches K, Angelini TG, Mudhar GS, Kaye J, Clark E, Bailey MA, Sohrabi S, Korossis S, Walker PG, Scott DJ, Porter KE: Exploring smooth muscle phenotype and function in a bioreactor model of abdominal aortic aneurysm. *J. Transl. Med.* 2013;11:208
10. Mao N, Gu T, Shi E, Zhang G, Yu L, Wang C: Phenotypic switching of vascular smooth muscle cells in animal model of rat thoracic aortic aneurysm. *Interact. Cardiovasc. Thorac. Surg.* 2015;21(1):62-70
11. Zaragoza C, Gomez-Guerrero C, Martin-Ventura JL, Blanco-Colio L, Lavin B, Mallavia B, Tarin C, Mas S, Ortiz S, Egido J: Animal models of cardiovascular diseases. *J. Biomed. Biotechnol.* 2011;2011:497841
12. Monk BA, George SJ: The effect of ageing on vascular smooth muscle cell behaviour - a mini-review. *Gerontology.* 2015;61(5):416-426

13. Ragnauth CD, Warren DT, Liu Y, McNair R, Tajsic T, Figg N, Schroff R, Skepper J, Shanahan CM: Prelamin A acts to accelerate smooth muscle cell senescence and is a novel biomarker of human vascular aging. *Circulation*. 2010;121(20):2200-2210
14. Wang M, Takagi G, Asai K, Resuello RG, Natividad FF, Vatner DE, Vatner SF, Lakatta EG: Aging increases aortic MMP-2 activity and angiotensin II in nonhuman primates. *Hypertension*. 2003;41(6):1308-1316
15. Michaud M, Balardy L, Moulis G, Gaudin C, Peyrot C, Vellas B, Cesari M, Nourhashemi F: Proinflammatory cytokines, aging, and age-related diseases. *J. Am. Med. Dir. Assoc.* 2013;14(12):877-882
16. Coppe JP, Desprez PY, Krtolica A, Campisi J: The senescence-associated secretory phenotype: the dark side of tumor suppression. *Ann. Rev. Pathol.* 2010;5:99-118
17. Porter KE, Naik J, Turner NA, Dickinson T, Thompson MM, London NJ: Simvastatin inhibits human saphenous vein neointima formation via inhibition of smooth muscle cell proliferation and migration. *J. Vasc. Surg.* 2002;36(1):150-157.
18. Turner NA, Aley PK, Hall KT, Warburton P, Galloway S, Midgley L, O'Regan DJ, Wood IC, Ball SG, Porter KE: Simvastatin inhibits TNF α -induced invasion of human cardiac myofibroblasts via both MMP-9-dependent and -independent mechanisms. *J. Mol. Cell. Cardiol.* 2007;43(2):168-176
19. Turner NA, Mughal RS, Warburton P, O'Regan DJ, Ball SG, Porter KE: Mechanism of TNF α -induced IL-1 α , IL-1 β and IL-6 expression in human cardiac fibroblasts: effects of statins and thiazolidinediones. *Cardiovasc. Res.* 2007;76(1):81-90
20. Riches K, Alshanwani AR, Warburton P, O'Regan DJ, Ball SG, Wood IC, Turner NA, Porter KE: Elevated expression levels of miR-143/5 in saphenous vein smooth muscle cells from patients with Type 2 diabetes drive persistent changes in phenotype and function. *J. Mol. Cell. Cardiol.* 2014;74:240-250
21. Riches K, Warburton P, O'Regan DJ, Turner NA, Porter KE: Type 2 diabetes impairs venous, but not arterial smooth muscle cell function: possible role of differential RhoA activity. *Cardiovasc. Revasc. Med.* 2014;15(3):141-8.
22. Madi HA, Riches K, Warburton P, O'Regan DJ, Turner NA, Porter KE: Inherent differences in morphology, proliferation, and migration in saphenous vein smooth muscle cells cultured from nondiabetic and Type 2 diabetic patients. *Am. J. Physiol. Cell Physiol.* 2009;297(5):C1307-C1317
23. Nilsson PM: Early vascular aging (EVA): consequences and prevention. *Vasc. Health Risk Manag.* 2008;4(3):547-552
24. Wilson WR, Herbert KE, Mistry Y, Stevens SE, Patel HR, Hastings RA, Thompson MM, Williams B: Blood leucocyte telomere DNA content predicts vascular telomere DNA content in humans with and without vascular disease. *Eur. Heart J.* 2008;29(21):2689-2694
25. Nelson G, Wordsworth J, Wang C, Jurk D, Lawless C, Martin-Ruiz C, von Zglinicki T: A senescent cell bystander effect: senescence-induced senescence. *Aging Cell.* 2012;11(2):345-349
26. Cafueri G, Parodi F, Pistorio A, Bertolotto M, Ventura F, Gambini C, Bianco P, Dallegri F, Pistoia V, Pezzolo A, Palombo D: Endothelial and smooth muscle cells from abdominal aortic aneurysm have increased oxidative stress and telomere attrition. *PloS One.* 2012;7(4):e35312

27. Thompson AM, Wagner R, Rzucidlo EM: Age-related loss of SirT1 expression results in dysregulated human vascular smooth muscle cell function. *Am. J. Physiol. Heart Circ. Physiol.* 2014;307(4):H533-H541
28. Vaziri H, Dessain SK, Ng Eaton E, Imai SI, Frye RA, Pandita TK, Guarente L, Weinberg RA: hSIR2(SIRT1) functions as an NAD-dependent p53 deacetylase. *Cell.* 2001;107(2):149-159
29. Badger SA, Jones C, McClements J, Lau LL, Young IS, Patterson CC: Surveillance strategies according to the rate of growth of small abdominal aortic aneurysms. *Vasc. Med. (Lond.).* 2011;16(6):415-421
30. Pei H, Tian C, Sun X, Qian X, Liu P, Liu W, Chang Q: Overexpression of MicroRNA-145 Promotes Ascending Aortic Aneurysm Media Remodeling through TGF-beta1. *Eur. J. Vasc. Endovasc. Surg.* 2015;49(1):52-59
31. Booth GL, Kapral MK, Fung K, Tu JV: Relation between age and cardiovascular disease in men and women with diabetes compared with non-diabetic people: a population-based retrospective cohort study. *Lancet (Lond.).* 2006;368(9529):29-36
32. Medema RH, Macurek L: Checkpoint recovery in cells: how a molecular understanding can help in the fight against cancer. *F1000 Biol. Rep.* 2011;3:10
33. Holt DJ, Grainger DW: Multinucleated giant cells from fibroblast cultures. *Biomaterials.* 2011;32(16):3977-3987
34. Shamanna RA, Hoque M, Lewis-Antes A, Azzam EI, Lagunoff D, Pe'ery T, Mathews MB: The NF90/NF45 complex participates in DNA break repair via nonhomologous end joining. *Mol. Cell. Biol.* 2011;31(23):4832-4843
35. Constantinescu D, Csoka AB, Navara CS, Schatten GP: Defective DSB repair correlates with abnormal nuclear morphology and is improved with FTI treatment in Hutchinson-Gilford progeria syndrome fibroblasts. *Exp. Cell Res.* 2010;316(17):2747-2759
36. Kinner A, Wu W, Staudt C, Iliakis G: Gamma-H2AX in recognition and signaling of DNA double-strand breaks in the context of chromatin. *Nuc. Acids Res.* 2008;36(17):5678-5694
37. Wan G, Mathur R, Hu X, Zhang X, Lu X: miRNA response to DNA damage. *Trends Biochem. Sci.* 2011;36(9):478-484
38. Fiedler J, Stohr A, Gupta SK, Hartmann D, Holzmann A, Just A, Hansen A, Hilfiker-Kleiner D, Eschenhagen T, Thum T: Functional microRNA library screening identifies the hypoxamir miR-24 as a potent regulator of smooth muscle cell proliferation and vascularization. *Antiox. Redox Sig.* 2014;21(8):1167-1176
39. Badi I, Burba I, Ruggeri C, Zeni F, Bertolotti M, Scopece A, Pompilio G, Raucci A: MicroRNA-34a induces vascular smooth muscle cells senescence by SIRT1 downregulation and promotes the expression of age-associated pro-inflammatory secretory factors. *J. Gerontol. A Biol. Sci. Med. Sci.* 2015;70(11):1304-1311

Figure Legends

Figure 1: Morphological features of aneurysmal SMC. Sub-confluent cells were cultured in full growth medium and imaged at x100 magnification. (A) AAA-SMC commonly exhibited granulation in the perinuclear region and often had a cytoskeleton that was visible under phase (arrows). SV-SMC and IMA-SMC did not exhibit these features. Representative images, with the previously described difference in cell size clearly evident [9]. Scale bar = 100 μm . (B) Cells were fixed and stained with rhodamine phalloidin to visualise the F-actin cytoskeleton (red). Nuclei were stained blue with DAPI. Truncated and disorganised F-actin filaments were apparent under both low (x200) and high (x630) magnification, whereas SV-SMC fibres were elongated and traversed the cells. Upper panel scale bar = 100 μm , lower panel scale bar = 20 μm . (C) and (D) The same analyses were performed on VEH-SMC and CCE-SMC from porcine carotid arteries maintained for 3 days in the bioreactor ('early stage'). Granulation and aberrant cytoskeletal features were very infrequent under any conditions. (E) and (F) Conversely, perinuclear granulation and truncation of the F-actin cytoskeleton was readily visible in CCE-SMC from 12 day bioreactor experiments ('end stage') compared to VEH-SMC.

Figure 2: Expression of markers related to DNA damage and senescence. SMC were cultured for 4 days in full growth media and RNA isolated. (A) Expression of SIRT-1, SIRT-3 and SIRT-6, all of which are known to decline in senescent cells (n=10, *P<.05, ns=non-significant vs. SV-SMC). (B) Expression of miR-145, a microRNA involved with DNA damage and that we have previously shown to be up regulated in senescent SMC from patients with type 2 diabetes [20] (n=12, ***P<.001 vs. SV-SMC or IMA-SMC). (C) and (D) In 'early' or 'end-stage' experiments, there was no difference in SIRT-1 or SIRT-3 expression amongst any conditions. SIRT-6 was not detected in porcine cells (n=3). (E) and (F) Expression of miR-145 was not affected by CCE in either 'early' or 'end-stage' experiments (n=3), in contrast to the increase seen in AAA-SMC.

Figure 3: Aneurysmal SMC display features of DNA damage. Sub-confluent cells were cultured in full growth medium and their nuclear morphology analysed. (A) The proportion of multi-nucleated cells in ~100 cells per patient were quantified (n=20, ***P<.001 vs. SV-SMC). Lower panel = representative images from AAA-SMC and SV-SMC with number of nuclei per cell indicated, scale bar = 100 μ m. (B) Cells were fixed and the proportion of aberrant nuclei in ~100 cells per patient counted (n=6, *P<.05 vs. SV-SMC). Lower panel = representative images from AAA-SMC and SV-SMC, scale bar = 50 μ m. Nuclei are stained with DAPI (yellow). Aberrant nuclei are denoted by an asterisk. (C) Cells were fixed and the proportion of ~150 cells per patient exhibiting double stranded DNA damage was quantified (n=6, ***P<.01 vs. SV-SMC). Lower panel = representative images from AAA-SMC and SV-SMC, scale bar = 100 μ m. DNA damage positive nuclei counterstain pink through co-localisation of γ H2AX (red) and DAPI (blue). (D-F) Identical experiments were performed on control and enzyme-treated porcine SMC from ‘early-stage’ experiments for (D) multi-nucleation (n=3, ns = non-significant vs. VEH-SMC), (E) nuclear morphology (n=3, ns = non-significant vs. VEH-SMC) and (F) γ H2AX-positive nuclei (n=3, ns=non-significant vs. VEH-SMC). (G-I) Identical experiments were performed on control and enzyme-treated porcine SMC from ‘end-stage’ experiments for (G) multi-nucleation (n=3, **P<.01 vs. VEH-SMC), (H) nuclear morphology (n=3, *P<.05 vs. VEH-SMC) and (I) γ H2AX-positive nuclei (n=3, ns=non-significant vs. VEH-SMC).

Figure 4: Correlation of chronological age with features associated with pathological premature ageing. (A) Age of patients whose SMC were used in this study (AAA-SMC n=31, SV-SMC n=57, ***P<.001). (B-F) Correlations of chronological age with markers of a pathological premature ageing phenotype in both AAA- and SV-SMC (B) SIRT-1, (C) miR-145, (D) multi-nucleation, (E) aberrant nuclear morphology, (F) γ H2AX-positive nuclei. Data were tested for normality using D’Agostino & Pearson omnibus normality test followed by

Pearson or Spearman correlation analysis as appropriate. r refers to the correlation between the two factors. All P values non-significant.

FIGURE 1 Riches et al.

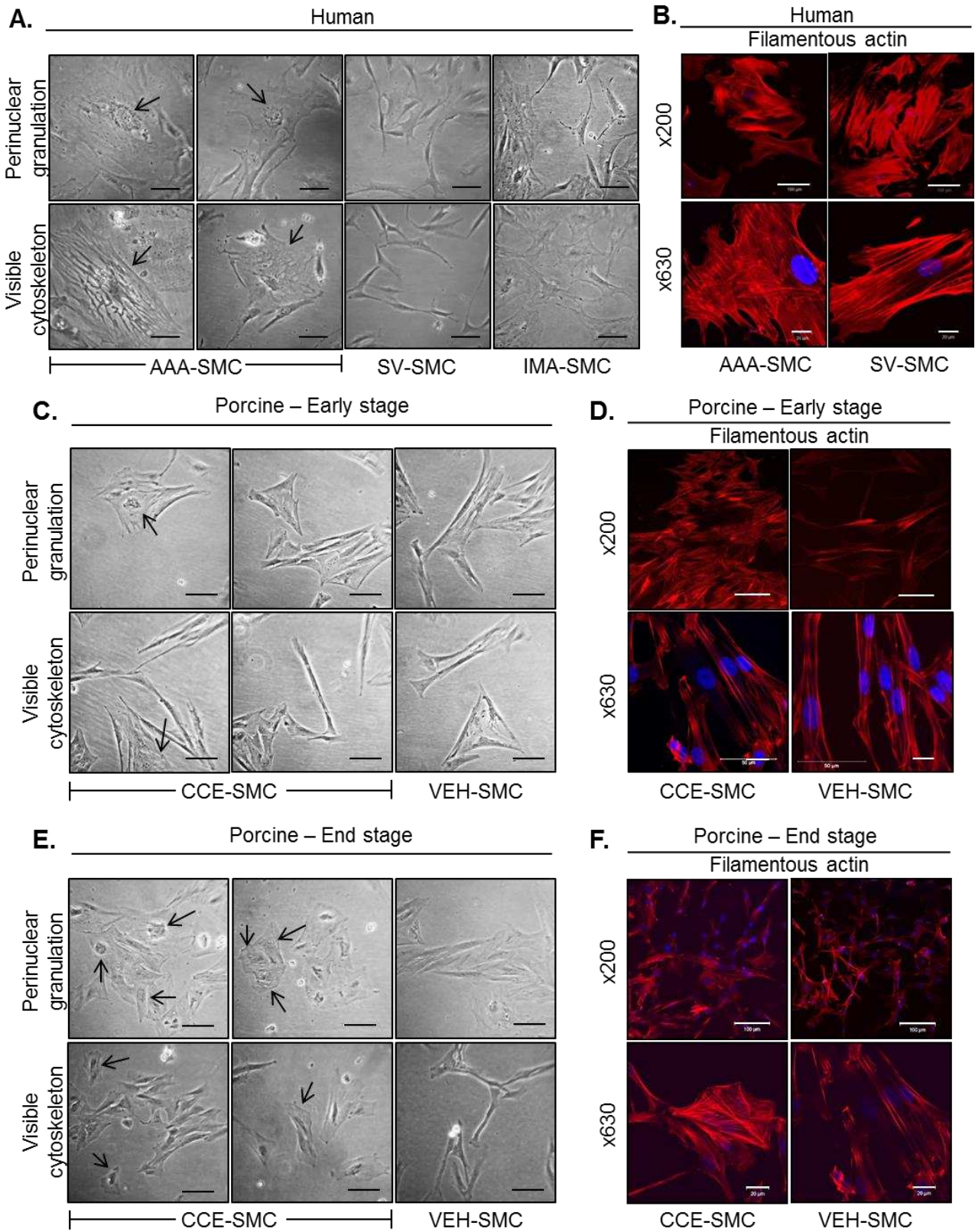


FIGURE 2 Riches et al.

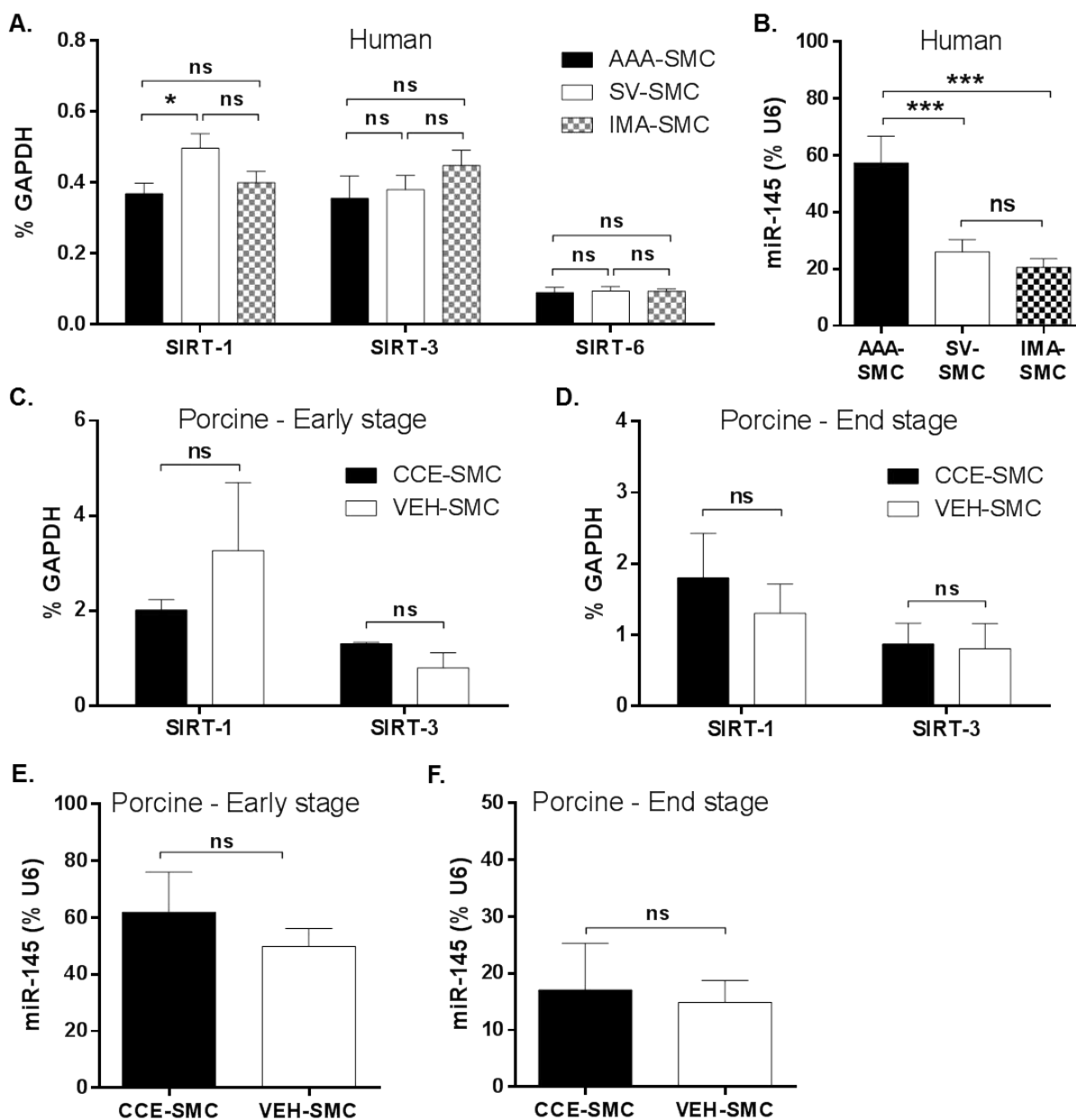


FIGURE 3 Riches et al.

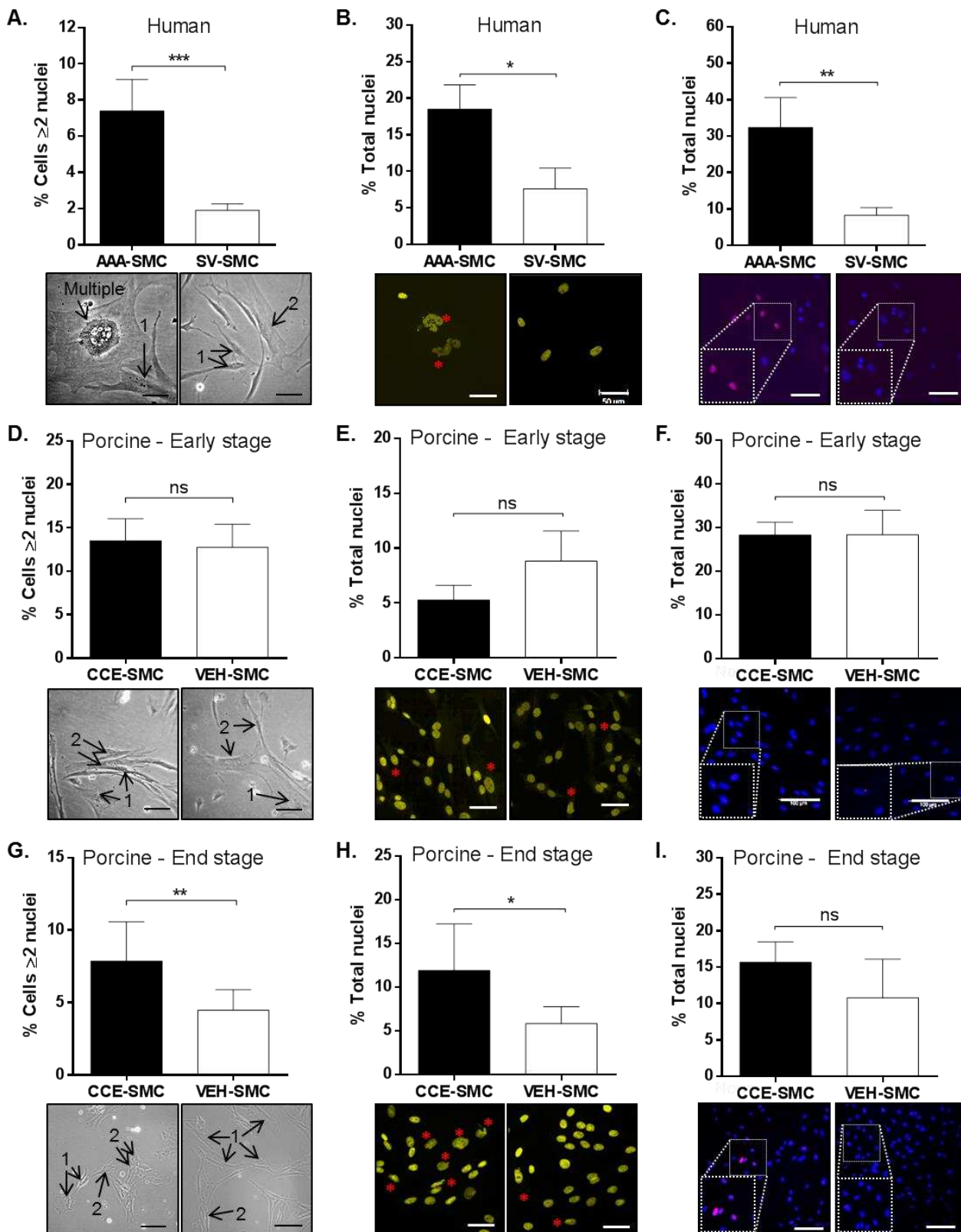


FIGURE 4 Riches et al.

